frontiers | Frontiers in Earth Science

TYPE Original Research
PUBLISHED 11 January 2023
DOI 10.3389/feart.2022.1096980

OPEN ACCESS

EDITED BY
Jun Zhao,
Anhui University of Science and Technology, China

REVIEWED BY
Yi Chang,
East China University of Technology, China
Feng Xu,
University of South China, China

*CORRESPONDENCE
Mingxin Zheng,
294817459@qq.com

SPECIALTY SECTION
This article was submitted to Geohazards and Georisks, a section of the journal Frontiers in Earth Science

RECEIVED 13 November 2022
ACCEPTED 05 December 2022
PUBLISHED 11 January 2023

CITATION
Fan Y, Zheng M and Wu J (2023), A study on the shear strength characteristics and microscopic mechanism of coal-bearing soil under dry-wet cycles. *Front. Earth Sci.* 10:1096980. doi: 10.3389/feart.2022.1096980

A study on the shear strength characteristics and microscopic mechanism of coal-bearing soil under dry-wet cycles

Yakun Fan[1,2], Mingxin Zheng[1]* and Junhua Wu[2]

[1]School of Transportation Engineering, East China Jiaotong University, Nanchang, China, [2]School of Civil Engineering and Architecture, Nanchang Hangkong University, Nanchang, China

The slope of coal-bearing strata distributed along the high-speed highway (railway) is affected by the atmospheric dry-wet cycles (DWC), and the collapse occurs many times during the construction of such highways, in Pingxiang city, in the province of Jiangxi. The DWC affect the strength characteristics of the unsaturated coal-bearing soil (CBS). In order to study the shear-strength characteristics of the unsaturated CBS under the DWC, the relationship between the shear strength and matric suction was analyzed by using direct shear test of the unsaturated CBS, the filter paper method of the matrix suction measurement, and the scanning electron microscope test. The internal reasons of shear strength attenuation of unsaturated CBS under DWC are revealed from microscopic perspective. The results show that the DWC at 0 to 4 times, with an increase in the water content, the clay domains expanded unevenly. Further, the clay minerals that served as the cementing junctions and soluble salts were softened and dissolved, and the bonding strength between the basic units and the cohesion of the samples decreased, so that the shear strength of unsaturated CBS samples decreased with an increase in the water content, and increased with the increase of matric suction. Under the influence of the DWC, the CBS samples slaked, the quartz matrix between the fissures slaked, and produce fragments and debris which reduced the size of large particles, and the bonding strength between the basic units was low. Therefore, the matric suction and the shear strength of the unsaturated CBS samples with the same moisture content, under the same normal pressure, decreased gradually with an increase in the number of the DWC. It is feasible to study the strength characteristics of unsaturated CBS by combining the test methods of macroscopic strength, matric suction and microstructure of soil.

KEYWORDS

dry-wet cycles, unsaturated coal-bearing soil, shear strength, matric suction, microstructure characteristics

1 Introduction

There are many coal-measure strata along the expressway (iron) road In Pingxiang City, in Jiangxi Province. Under the action of the atmospheric DWC, the slope of coal measure strata in expressway (railway) has collapsed many times during construction (YANG and ZHENG, 2018). The coal-measure strata and its weathered materials are generally referred to as the CBS, which are characterized by uneven soft and hard soil layers, poor interlayer cementation, loose structure, fast weathering speed after excavation, softening, disintegration, and loss of strength in the event of water-saturation (Han et al., 2019). Therefore, it is of great theoretical and practical significance to study the engineering properties of the unsaturated CBS under the DWC for slope stability and soil and water conservation.

The shear strength theory of the unsaturated soil has been studied for several decades, amongst which the most accepted shear strength formulae for the unsaturated soil are the Bishop effective stress strength formula (BISHOP and BLIGHT, 1963) and the Fredlund double stress variable strength formula (FREDLUND et al., 1978), both of which reflect the contribution of the matric suction against the shear strength. Due to the difficulties in measuring and calculating the matric suction, many studies have chosen the water content or the saturation to replace matric suction in the study of the unsaturated soil strength (Cui and Si, 2014; Aqtash and Bandini, 2015; Hassan Marwan Adil and Mohamad Ismail Mohd Ashraf, 2018; Qian et al., 2020; Ma, Huang, Hu, Yang; Chou and Wang, 2021). However, some studies have pointed out that there is no one-to-one single value relationship between the matric suction and the water content in unsaturated soil strength. Chengren (XIONG et al., 2005) discussed the variation characteristics of matric suction in the unsaturated soil water-density state space, and discovered that there was neither direct correlation nor definite corresponding relationship between the matric suction and saturation, but that water and the soil structure were two very important factors affecting the matric suction. Therefore, matric suction is a combination of water content and soil structure, which is more suitable for the analysis of the shear properties of the unsaturated soils. Changguang et al. (ZHANG et al., 2012) divided the various unsaturated soil shear strength formulas into five categories, among which the formula index of the total stress shear strength has been widely used in practical engineering. Therefore, with a change in the moisture content and the soil structure of the CBS, the filter-paper method could be used to transform the measured matric suction into the total stress shear strength of the soil, which has high application value in engineering practices.

The macroscopic physical and mechanical properties of the rock and soil as well as their specific engineering properties all depend on their microscopic structure (Zuo et al., 2016; NOWAMOOZ et al., 2016; Zhao et al., 2018; Zhou et al., 2021). However, most studies have focused on the micro-structure of the red clay, expansive soil, loess, and silty sand (ALDAOOD et al., 2014; Jiang et al., 2014; AHMED, 2015; Lin and Amy, 2015; Sun and Cui, 2018; Xiao et al., 2020; Wang et al., 2021), for instance. Some studies had also investigated the slope protection and the reinforcement of the CBS, the physical and the mechanical properties of the soil, and the micro-structure parameters (Hang et al., 2019; Huang and Zheng, 2021; Zhang et al., 2021). There are few studies, however, on the relationship between the microstructure and the macroscopic strength of the unsaturated CBS under the wetting and drying cycles. In this paper, the remolded samples of the CBS along the Changli Expressway were taken as the research object. Based on the total stress strength, the shear strength, and the microstructure characteristics, the unsaturated CBS under the dry and wet cycling conditions were studied by the direct shear test of the unsaturated CBS, matrix suction test by the filter-paper method, and the microscopic scanning electron microscope test. The relationship between the shear strength and the matric suction of the unsaturated CBS was analyzed, and the cause of the shear-strength attenuation of the unsaturated CBS under the three DWC was revealed from the microscopic point of view, which provided some important and beneficial supplements for the study of engineering properties of the unsaturated CBS and slope stability.

2 Methods

2.1 Basic characteristics of the test soil samples

The CBS used in this test was taken from the landslide soil in K213 section of the Changli Expressway in Jiangxi Province. The specific physical and mechanical indexes are shown in Table 1.

The particle composition of the CBS is shown in Table 2. According to the classification of soil of the Highway Geotechnical Test Regulations, the CBS belongs to clay-sand.

2.2 Testmethod

2.2.1 Soil samplepreparation

According to the compaction degree of the 93% of the maximum dry density of the compaction test, the CBS sample with the dry density of 669.1 g/cm^3 was prepared. In this paper, the particles of the remolded samples were all passed through a 2 mm screen, and the prepared soil was pressed into a large round sample with a diameter of 100 mm, and a height of 40 mm by the sample pressing method. Then the samples were placed on a water tray, and soaked and saturated with the water absorption by using the principle of the capillary water absorption. In the indoor constant temperature (20°C)

TABLE 1 The main physical and mechanical indices of the CBS as used in this study.

Specific gravity	Liquid limit	Plastic limit	Maximum dry density (g/cm3)	Optimum moisture content (%)
2.68	31.8	17.8	1.795	18.36

TABLE 2 The particle gradation of the CBS.

Particle size/mm	2	1	0.5	0.25	0.075
The percentage of particles smaller than the particle size to the total weight (%)	100	94.8	78.3	64.6	29.5

X-ray diffraction analysis showed that the mineral composition of the sample is mainly quartz, muscovite, and calcium carbonate, but also contains a small amount of kaoliniteand chlorite (about 18%).

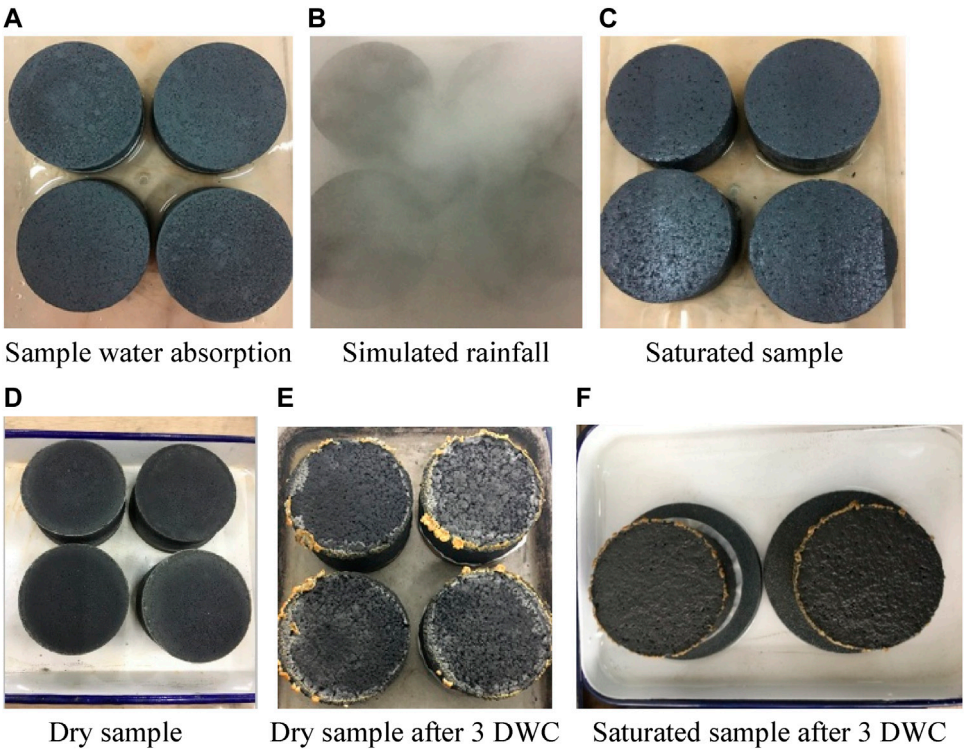

FIGURE 1
The surface morphology of the large round samples with the hygroscopic, dehumidifying, and after three DWC. **(A)** Sample water absorption **(B)** Simulated rainfall **(C)** Saturated sample **(D)** Dry sample **(E)** Dry sample after three DWC **(F)** Saturated sample after three DWC.

environment, the water loss was simulated by blowing the saturated sample surface with miniature electric fan. The mass of the unchanged CBS sample indicated that the dehumidification was finished. Then in the test, a humidifier was used to spray the surface of the sample, and the capillary action was used to make the bottom surface of the sample absorb water to simulate the process of the rain-moisture absorption. When the mass of the CBS sample did not increase, the water spraying was stopped, and the plastic film was used to seal it for at least 24 h. The repeat cycles of DWC were also performed. Figure 1 shows the surface morphology of the large round sample of the CBS prepared by the sample pressing method after hygroscopicity, dehumidification, and three DWC.

2.2.2 Test plan and procedure

There were five DWC in this study, and the moisture content of the coal-measure soil samples in eachDWCwere 21%, 17%, 13%,

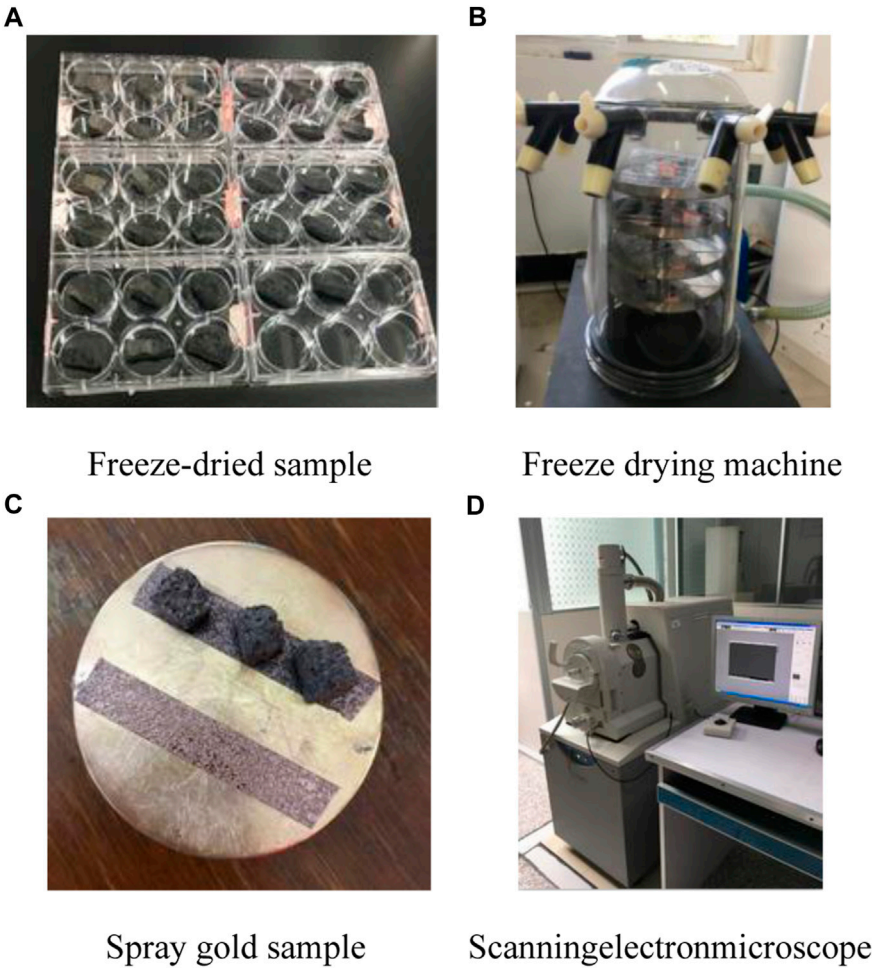

FIGURE 2
The matric suction test sample **(A)**. Freeze-dried sample **(B)**. Freeze drying machine **(C)**. Spray gold sample **(D)**. Scanning electron microscope.

and 9%, with four samples in each group. A small ring knife was used to take samples from the large round samples, and the remaining intact samples were preserved with plastic film for the scanning electron microscope test. The samples were placed in the direct-shear instrument, and the overlaying loads of 50 kPa, 100 kPa, 150 kPa, and 200 kPa were applied until the deformation was stabilized, and the undrained, fast shear was carried out at the constant shear rate of 0.013 mm/s. After the direct shear test, the matrix suction value was measured by the filter-paper method, along the shear plane, which was approximately the average suction of the sample in the shear process. The soil samples retained for the scanning electron microscopy tests were gently broken into strips of soil about 15 mm and 10 mm wide, and then frozen in a—80°C refrigerator for more than 36 h to make the pore water in the soil become amorphous ice without the volume expansion. The samples were then treated by the freeze-vacuum sublimation drying method, and the dried samples were sprayed with gold before the scanning electron microscope test. The soil samples and instruments were tested in each step, as shown in Figure 2. Images with magnification of 2000 times were uniformly selected for this study.

3 Test results and analysis

3.1 The shear strength

In this test, the unsaturated CBS samples were subjected to undrained fast shear, so the shear strength obtained was the total stress strength. Figure 3 shows that there is a linear relationship between the shear strength and the normal stress of the unsaturated CBS samples under the different wetting and drying cycles. In the same drying-wetting cycles, the shear strength of the unsaturated CBS samples decreases gradually with the increase of the moisture content. When the normal stress of the 0 drying-wetting cycle was 200 kPa, and the moisture content increased from 9% to 21%, the shear strength of the

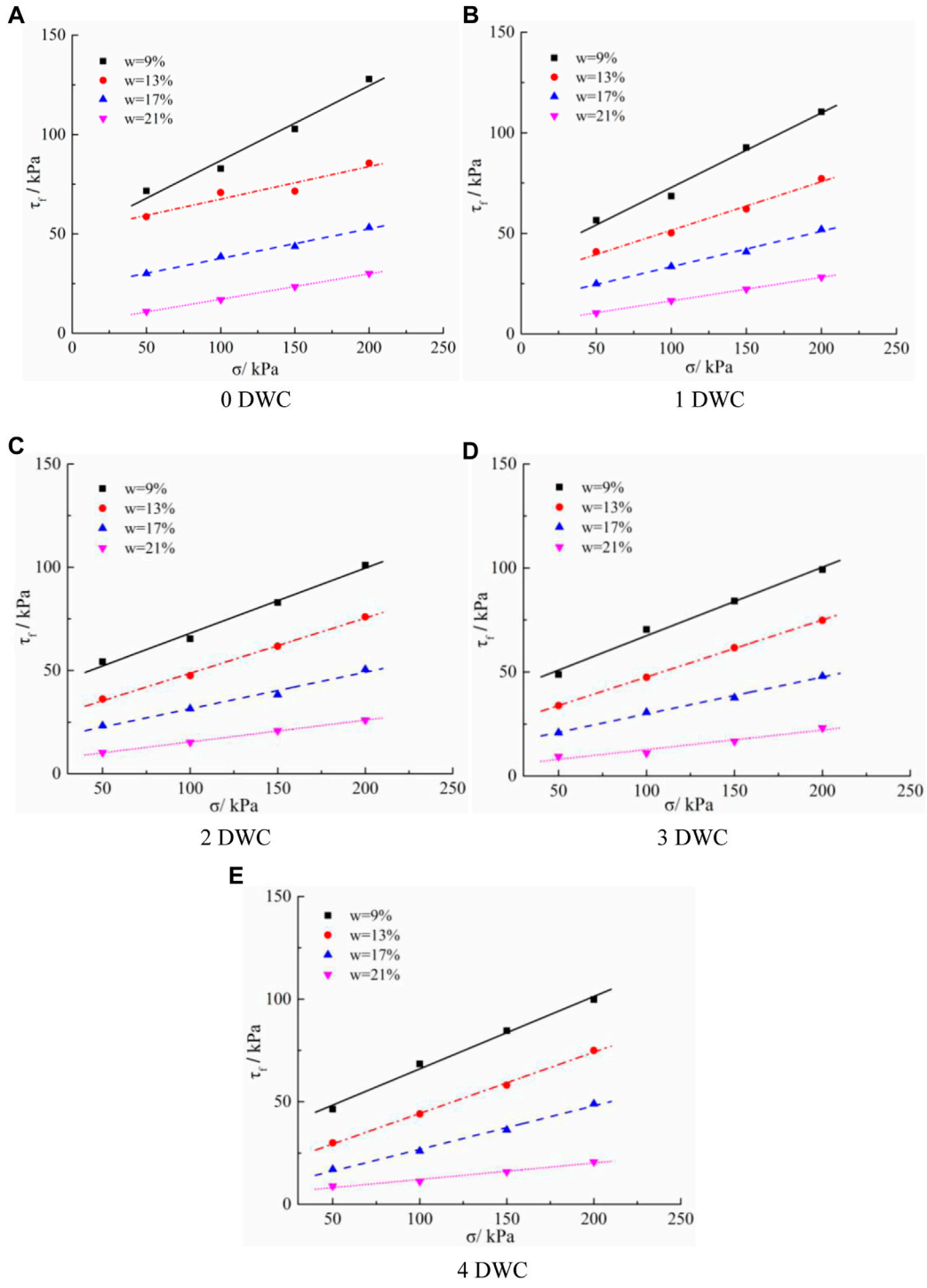

FIGURE 3
Relationship between the shear strength and the normal stress of samples with the different water contents **(A)**. 0 DWC **(B)**. One DWC **(C)**. Two DWC **(D)**. Three DWC **(E)**.Four DWC.

unsaturated CBS samples decreased from 128 kPa to 30 kPa, respectively, which reflects a reduction by 77%. In addition, the shear strength of the soil increased with the increase of the normal stress under the same drying-wetting cycles and the same moisture content. For example, when the normal stress increased from 50 kPa to 200 kPa, the shear strength of the soil with 9%

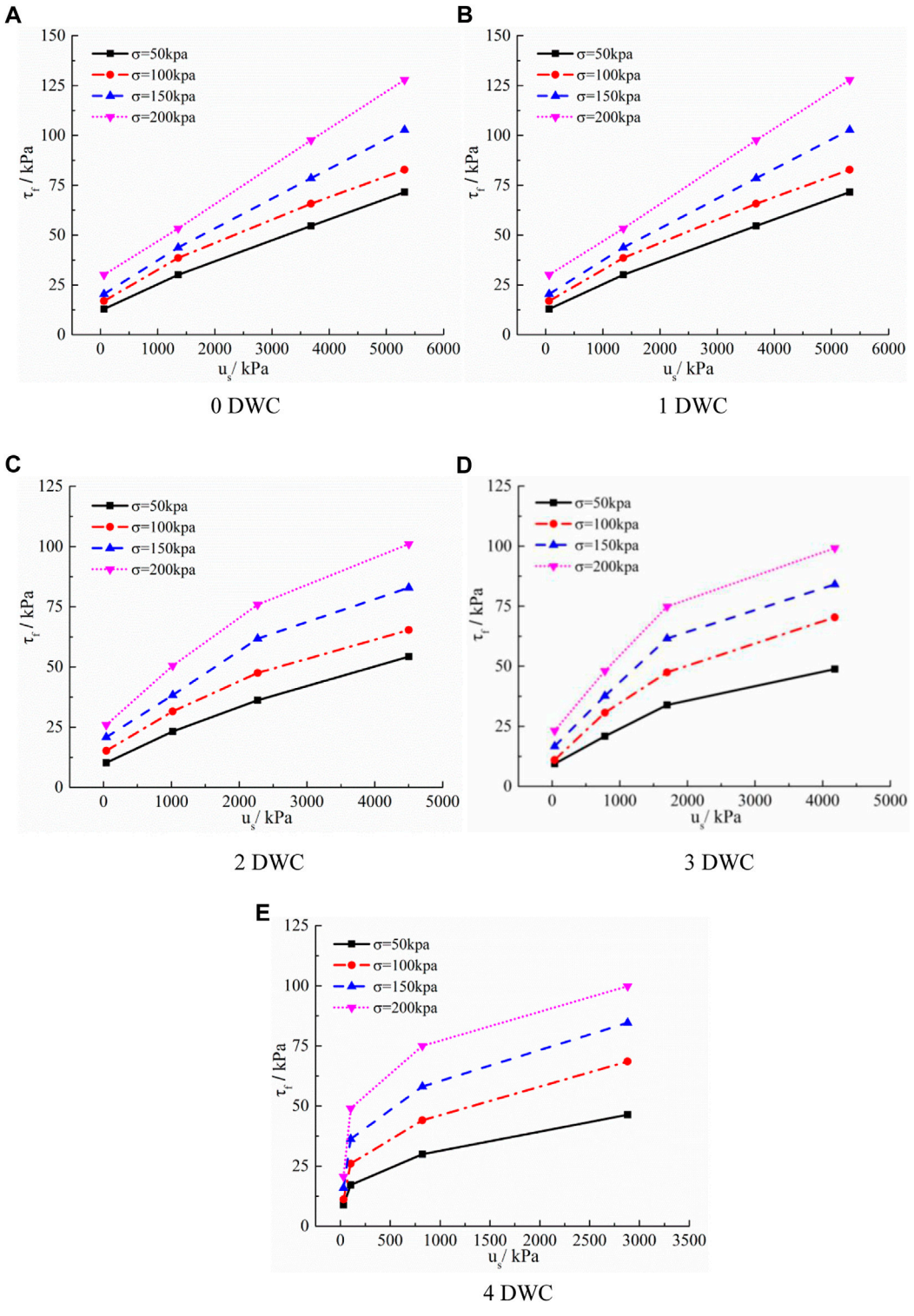

FIGURE 4
Relationship between the shear strength and the matric suction of the samples under the different DWC **(A)**. 0 DWC **(B)**. One DWC **(C)**. Two DWC **(D)**. Three DWC **(E)**. Four DWC.

TABLE 3 The total stress shear strength indices and the matric suction of the samples under the different DWC.

The number of wet and dry cycles/*n*	The moisture content /%	$c_{total}/(kPa)$	$\phi_{total}/(°)$	The matrix suction $/(kPa)$
1	9	30.7	19.4	2,880.6
	13	14.5	16.6	821.8
	17	5.6	12.0	103.3
	21	4.1	4.6	31.0

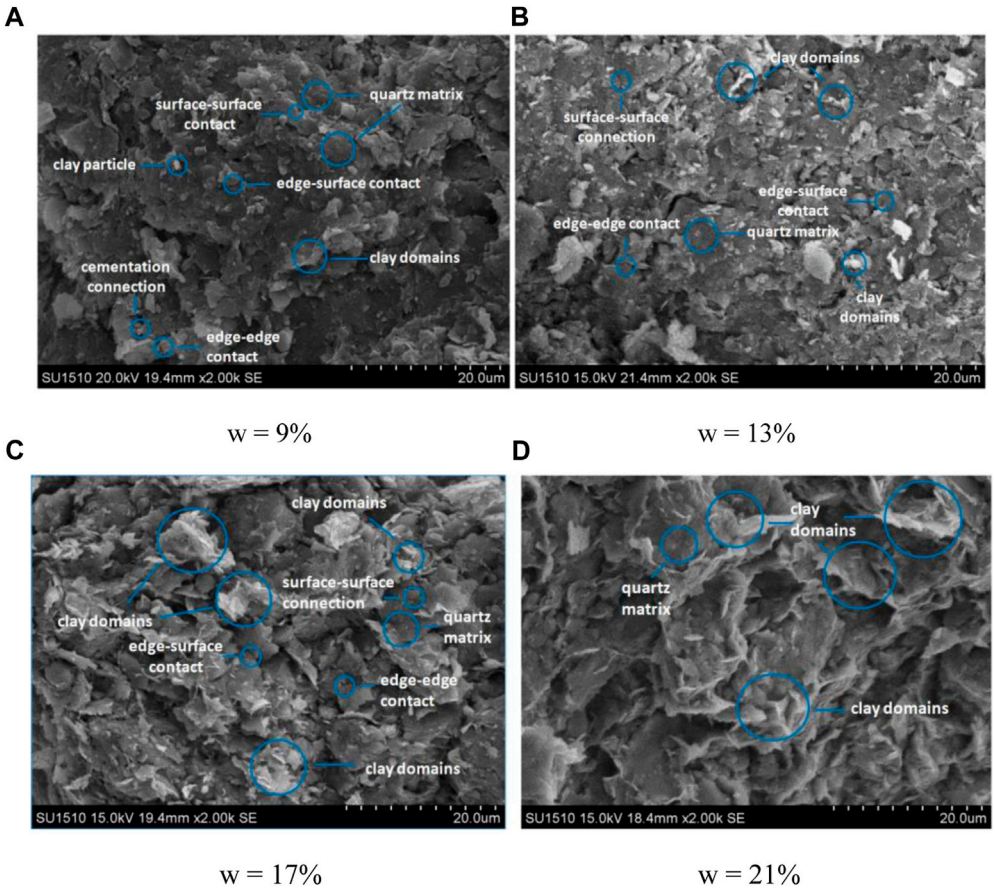

FIGURE 5
The 0 DWC microcosmic structures of the CBS with the different moisture contents. **(A)** w = 9% **(B)** w = 13% **(C)** w = 17% **(D)** w = 21%.

moisture content for 0 drying-wetting cycles increased from 72 kPa to 128 kPa. The shear strength of the unsaturated CBS samples, with the same moisture content, decreased with the increase of the number of the drying and wetting cycles. For example, for the unsaturated CBS samples with a moisture content of 9% undergoing 0–4 drying-wetting cycles, when the normal stress was 200 kPa, the shear strength was 128 kPa, 110 kPa, 101 kPa, 99 kPa, 100 kPa.

3.2 The influence of the matric suction on the shear strength

Linchang et al. (MIAO et al., 2000) reformulated the expression for the shear strength of the unsaturated soil, into a strength formula similar to Mohr-Coulumb (Eq. 1, as follows):

$$\tau_f = c_{total}(u_s) + \sigma \tan \psi_{total}(u_s) \quad (1)$$

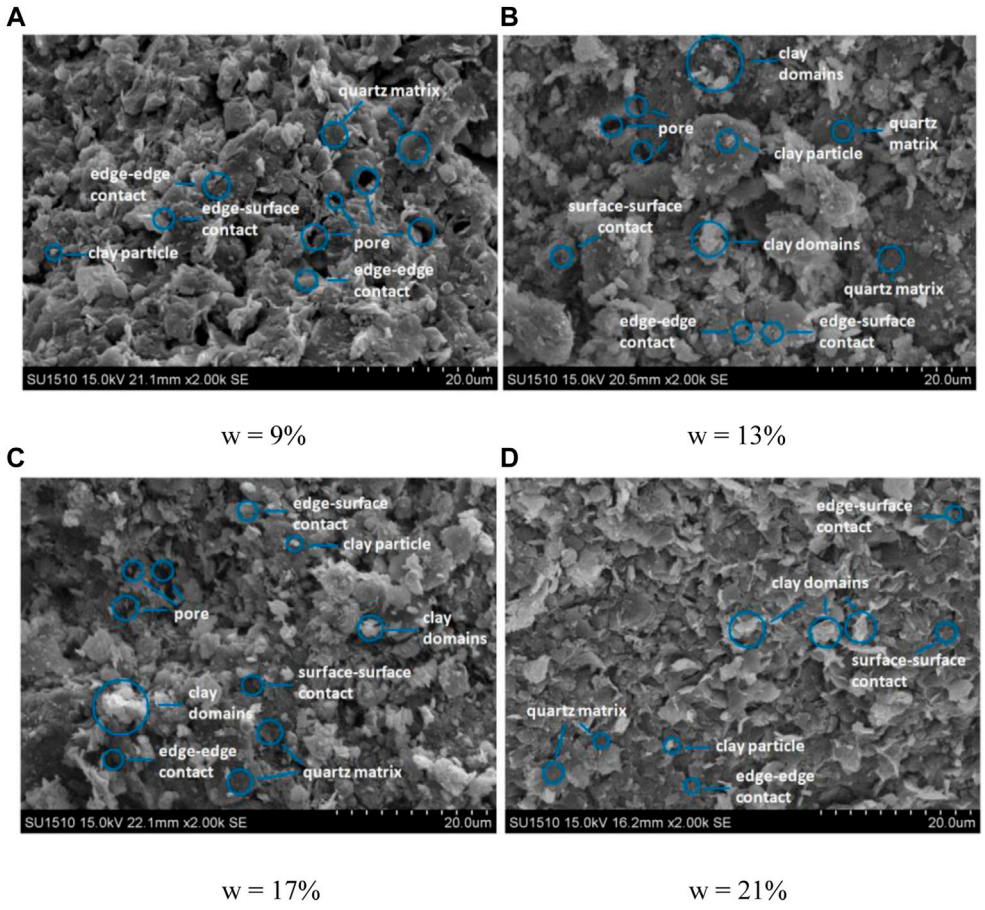

FIGURE 6
The three DWC microcosmic structures of the CBS with the different moisture contents. **(A)** w = 9% **(B)** w = 13% **(C)** w = 17% **(D)** w = 21%.

where, τ_f is the total stress shear strength; c_{total} is total cohesion; ψ_{total} is the total internal friction angle; u_s is the matrix suction. The shear strength obtained in this test is the total stress shear strength, the cohesion of soil is the total cohesion, and the friction angle is the total internal friction angle. Figure 4 shows the relationship between the total stress shear strength and the matric suction of the coal-measure soil samples under the different normal stress conditions and different DWC. Over the DWCconditions at the same time, the sample shear strength which increased with the increase of the matrix suction, including the zero DWC, when the increase of the matrix suction influence on the strength of soil increased more clearly, the approximate to linear, the influence of matric suction on the soil strength increases gradually during one to four DWC. In addition, in the same DWC, the corresponding shear strength of the matrix suction was different when the matrix suction was the same, indicating that the contribution of the matrix suction to the shear strength was different when the stress environment was different. The shear strength increased with the increase of the normal stress applied to the coal measure soil sample. Under the different drying and wetting cycles, the matric suction and the shear strength of the soil samples with the same moisture content, under the same normal pressure, gradually decreased with the increase of the number of drying and wetting cycles, indicating that there was no definite one-to-one correspondence between the water content or the saturation and the matric suction. The contribution of the matric suction to shear strength was influenced by the change of the soil structure and the water content after the repeated DWC. And along with the rise of DWC times, the coal-soil structure changed in the matrix suction and the influence of the shear strength, than the effects of the moisture content, change was bigger, which makes it consistent with the conclusions as in a previous study (Fu et al., 2019), The changes, namely, in the DWC and the repeated wetting and drying cycles, affect the wetting shear strength of the soil more than the water content, which, in turn, is only caused due to the changes brough about in the structure of the soil.

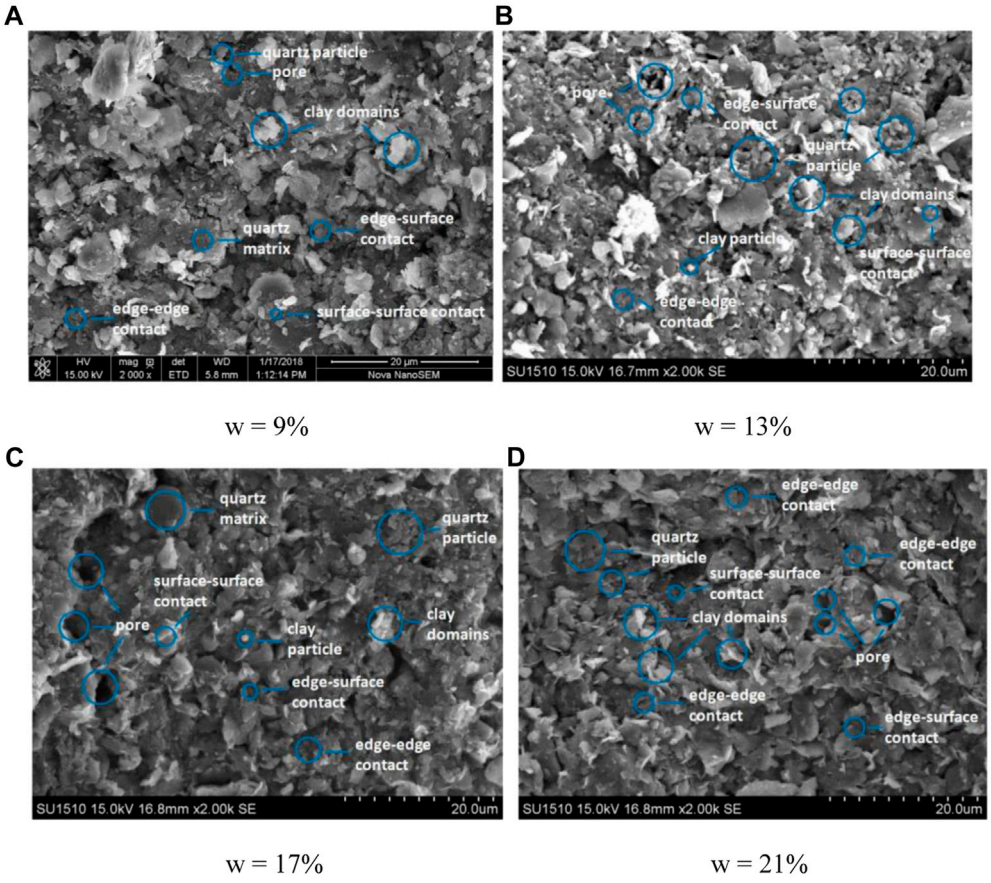

FIGURE 7
The four DWC microcosmic structures of the CBSwith the different moisture contents. **(A)** w = 9% **(B)** w = 13% **(C)** w = 17% **(D)** w = 21%.

Table 3 shows the total stress shear strength index and matric suction of coal measure soil under different drying and wetting cycles. It can be seen that there is a linear relationship between the total stress shear strength index and the logarithm value of matric suction under each drying and wetting cycle. Therefore, the shear strength model of unsaturated coal measure soil under drying and wetting cycle is as follows (Eq. 2):

$$\tau_f = (a + b\lg u_s) + \sigma \tan(c + d\lg u_s) \quad (2)$$

where, a, b, c,d are the fitting parameters of c_{total}, ψ_{total} and matrix suction respectively.

3.3 Analysis of microstructure characteristics

The influence of the soil structure on the matric suction and shear strength of the CBS is greater than that of water content under the DWC. The change in the soil structure at the macro level is reflected in the change of soil structure at micro level. The DWC with the zero moisture content 9% of the coal-soil sample in the scanning electron microscope (SEM) image (Figure 5) show that the quartz-particle plate-shaped structure form the soil sample matrix, the matrix surface has cracks, and form a particle size difference than that of the of quartz grains, the kaolinite and the chlorite form the clay particles in the clay domain, which are in the form of surface to surface connection attached to the surface of the quartz substrate, or in the form of surface to surface connection in the quartz matrix in the cracks and in the quartz-particle joints. The lamellar quartz particles are mainly edge to edge, edge to surface, and surface to surface contact. The interface between the aggregates formed by the clay domain surface to surface contact and the quartz particles is mainly edge to surface, surface to surface contact. The connection is cemented by clay minerals and soluble salts, or the contact connection is formed by the direct contact between the basic

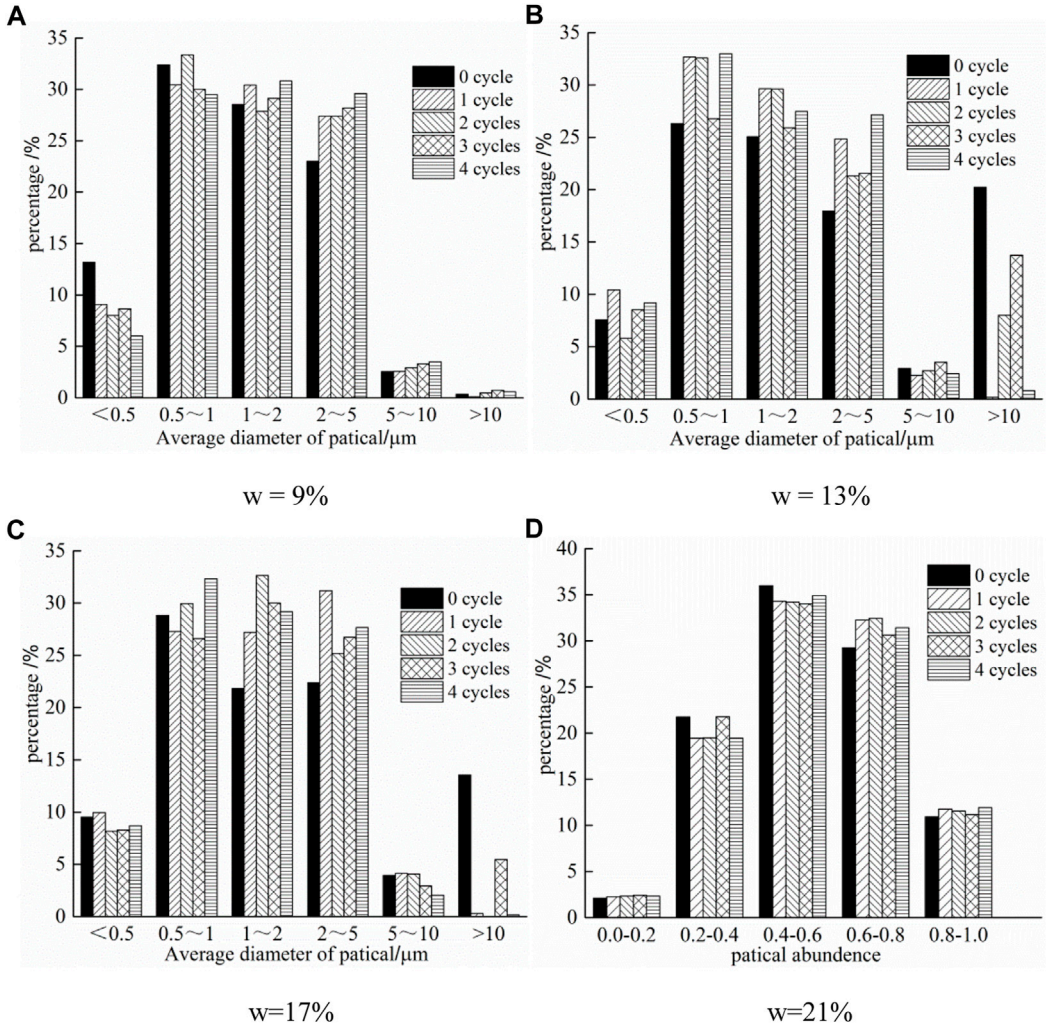

FIGURE 8
The variation of average diameter percentage of the soil particles under different DWC **(A)** w = 9% **(B)** w = 13% **(C)** w = 17% **(D)** w = 21%.

units. At this time, the cementation strength between the basic units is not high, and the particle connection is relatively loose. The SEM images (Figure 5) of the CBS samples with the moisture contents of 9%, 13%, 17%, and 21% during the 0 cycle of wetting and drying show that with the increase of the moisture content, the particle morphology, and the connection between the particles of the samples changed. The overlap formed by the facetoface contact of the clay expands with the increase of water content in the soil. Long, flat, clay domains with thick middle and thin edges are observed on the surface of the quartz matrix, between the cracks, and the quartz grains. This happened because the surface of the clay domain is generally negatively charged, while the connection between the surface-and-surface of the clay domain is mainly ion-electrostatic. As the water in the soil increased, the water film thickened, the diffusion-double electric layer thickened, and the repulsion between the surface-and-surface predominated, resulting in the expansion of the polymer. With the increase of the water content, the cemented clay minerals, and the soluble salts at the junction of the basic unit body softened and dissolved. At this time, the cementation strength between the basic unit body decreased greatly, and the cohesion of the sample somewhat decreased. In the scanning electron microscope images of the samples with different moisture content in the first, second, third, and the fourth drying and wetting cycles (see Figures 6, 7 for the third and fourth dry and wet cycles), it can also be observed that the uneven volume expansion of the clay domain occurs with the increase of the water content, and the clay minerals and soluble salts that play the role of cementing connection softened and dissolve. Further, the basic unit body and the change of the pore volume caused the gas-liquid interface in the change of the

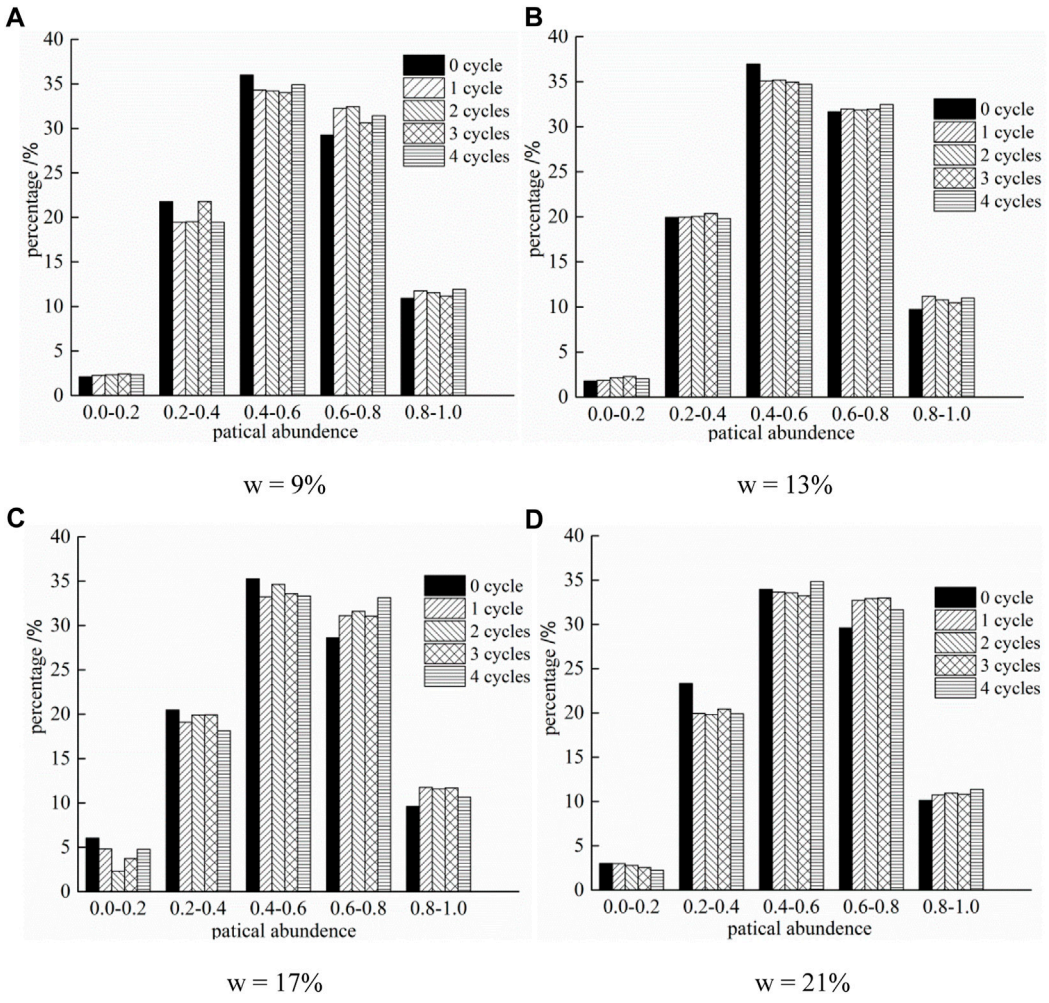

FIGURE 9
The variations of the soil particle abundances under the different DWC. **(A)** w = 9% **(B)** w = 13% **(C)** w = 17% **(D)** w = 21%.

meniscus water film, which caused the change of the matrix suction. It was at the same time during the drying-wetting circulation process, that the soil specimen macro performance of the shear strength of the unsaturated coal decreased gradually with the increase of the moisture content, and with the increase of the matrix suction, which can all be seen microscopically.

With the 0, 1, 2, and 3 times of the DWC, the moisture content is 9%, 4 times of the coal-soil sample in the electron microscope scanning figures. With the increase of the DWC, collapse happened in the coal soil sample, the cracks of the quartz substrate collapse happened, the magnitude of the large particle size decreased, and the clay minerals content in the DWC under the influence of particle size reduced. Further, the cementation strength between the basic units decreased, the particle connections became looser, and there were more pores. This is also the microscopic reason that the matric suction and the shear strength of the unsaturated CBS samples with the same moisture contents, and under the same normal pressure gradually decreased with the increase of the number of DWC.

3.4 The influence of the drying and wetting cycles on the characteristic parameters of the microstructure

The image processing software IPP (Image-Pro Plus) was used to analyze and process the SEM images of the CBS with different water contents after 0–4 DWC, and the microstructure information was extracted to analyze the average particle average of the CBS after different DWC. The changes in the microstructural characteristic parameters, such as the diameter, particle abundance, and the particle orientation frequency were examined.

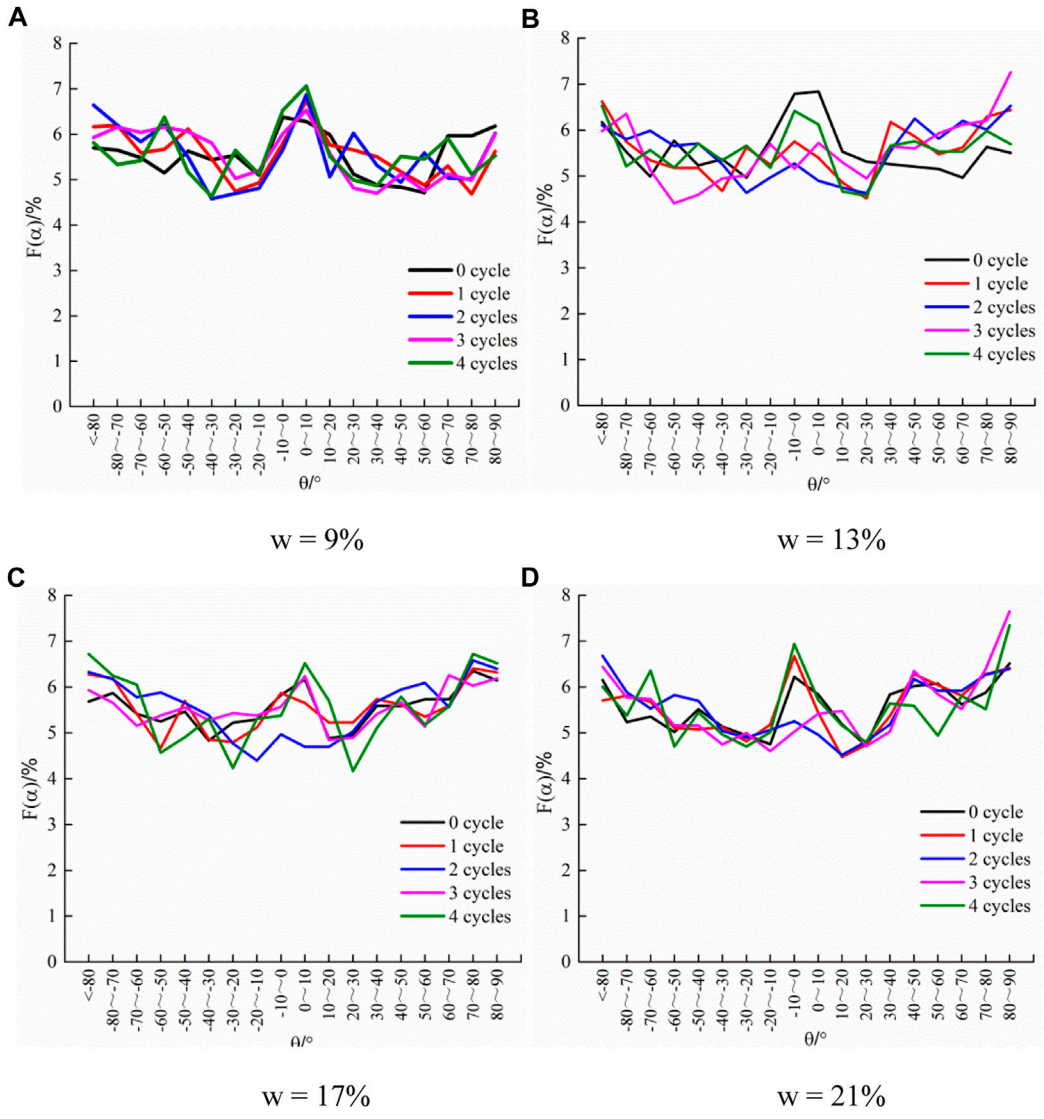

FIGURE 10
The directional frequency of the soil particles under the different DWC. **(A)** w = 9% **(B)** w = 13% **(C)** w = 17% **(D)** w = 21%.

3.4.1 The average particle diameter

The average particle diameter was used to represent the particle size. The diameter of the circle is equal to the particle area, S, and where Dis the average diameter of the particle unit body. The calculation formula is (Eq. 3):

$$D = \sqrt{\frac{4S}{\pi}} \tag{3}$$

The average particle diameter was classified over a certain range, and the percentage of the number of particles in each interval of the soil samples with the different moisture contents under the different DWC was counted, and the results are shown in Figure 8.

For the CBS with the moisture content of 9% and 13% under the different drying and wetting cycles, and with the increase of the drying and wetting cycles, the particle size was less than 0.5 μm and between 0.5 ~ 1 μm, respectively. The content of the particles between1 ~ 2 μm and 2 ~ 5 μm, however, was in an increasing state, the content of particles between 5 ~ 10 μm did not change much, and the content of particles larger than 10 decreased. For the CBS with the moisture content of 17% and 21%, under the different DWC, and with the increase of DWC, the content of particles with the particle size of less than 5 μm was in an

increasing state, and the content of particles with the particle size over five to 10 μm did not change much. The content of the particles with the diameter greater than 10 μm decreased. This was mainly related to the disintegration of the CBS samples after the multiple DWC. As the number of DWC increases, the content of particles with a particle size of less the than five increased, the disintegration and the dispersion of the large particles reduced their contents. The contents of the small particles increased when the moisture content was lower, however, and the smaller particles adhered to the larger particles, which formed a larger particle, and which reduced the percentage of the smaller particles over this range. Yet, when the same is high, the number of the DWC and the high water content weakened the cementation between the basic units, the particle connection was weaker, and the particles were more loose, so that the content of particles in the range of less than 5 μm particles increased.

3.4.2 Particle abundance

The ratio of the short axis to the long axis of the particle is the particle abundance C, and its calculation formula is (Eq. 4):

$$C = \sqrt{\frac{B}{L}} \tag{4}$$

where B is the short axis of the particle, and L is the long axis of the particle. The value of C ranges from 0 to 1, and the closer C is to 1, the more circular the particles tend to be on the plane, and the more elongated they tend to be.

Figure 9 shows the particle abundance of the reconstituted CBS with the different water contents under the different DWC. With the increase of the number of DWC, the abundance percentage of the particles with abundance less than 0.6 gradually decreased, while the abundance percentage of the particles with abundance greater than 0.6 showed an increasing trend, indicating that the effect of the DWC gradually changed the shape of the particles. From long strips to that of approaching the circle. Under the action of the multiple DWC, the quartz matrix of the CBSsample disintegrated, and the clay minerals dispersed and disintegrated, so that the size of large particles decreased more, the number of the small particles increased, and the particles with the complex shapes tended to be simple, which resulted in the soil erosion.

3.4.3 The particle orientation frequency

The particle orientation frequency is the frequency at which the angle between the long axis and the X axis of the particle is calculated into each equally divided orientation angle interval. The orientation angle interval is at $\Delta\theta = 20$, divide 180° into nine orientation angle intervals, and $F_i(\alpha)$ represents the orientation frequency of the particle unit in ith orientation angle interval (Eq. 5):

$$F_i(\alpha) = \frac{n_i}{n} \tag{5}$$

where n_i is the number of particles whose long axis direction falls in ith orientation angle interval, and n is the total number of particles.

It can be seen from Figure 10 that the orientation angle of the reshaped coal measures soil particle unit has a certain distribution in each interval, but it is mainly concentrated in the interval of −10°–10z, that is, the particles are mainly arranged in the horizontal direction and have a certain orientation. With the increase of the number of the drying and wetting cycles, the orientation frequency of the particle units increased significantly in the range of −10°–10°. The percentage content was the highest, while the variation law of orientation frequency in other orientation angle ranges is not apparent. The remolded CBS was prepared by the compaction method. During the compaction process, the soil particles were arranged in the horizontal direction under the action of the vertical force, that is, the angle between the main axis of the particle unit and the X axis was in the horizontal direction and. −10°–10° range. Under the action of the DWC, the disintegration and the dissolution of the coal-measure soil increased the number of the soil particles, decreased the average particle diameter, weakened the inter-particle cementation, and changed the contact mode between the particles, which affected the soil mass to a large extent. Cohesion, soil particles are more loose, and the arrangement of particle units tends to be simpler and orderly.

4 Conclusion

1) In 0 to four DWC, the clay domain expands unevenly with the increase of water content, the clay minerals and soluble salts that play the role of cementation and connection soften and dissolve, the cementation strength between basic units decreases greatly, the cohesion of the sample decreases, and the changes of water, basic units and pores cause the changes of meniscus water film at the gas-liquid interface, thus causing the changes of matrix suction, The shear strength of unsaturated CBS sample decreases with the increase of water content in the same DWC, and increases with the increase of matrix suction.
2) The CBS samples disintegrated under the action of DWC, and the quartz matrix in the cracks disintegrated to produce fragments and debris, and the particle size of large particles decreased more. The diameter was also reduced, the disintegrated and dispersed particles were scattered on the surface of the quartz matrix and around the other particles

and in the pores. The same was more loose and had more pores, so that the matrix suction and the shear strength of the unsaturated CBS samples with the same water content under the same normal pressure condition gradually decreased with the increase of the number of DWC.

3) Under the action of the DWC, the disintegration and dissolution of the CBS increased the number of the soil particles, reduced the average particle diameter, changed the particle shape, weakened the inter-particle cementation, and changed the contact mode between the particles. It is shown here that the content of the particles with the average diameter of less than 5 μm increased, while the content of the particles larger than 10 μm decreased. The shape of the particles gradually approached from a strip to a circle, while the particle orientation was slightly more apparent.

Data availability statement

The original contributions presented in the study are included in the article/supplementary material, further inquiries can be directed to the corresponding author.

Author contributions

YF: Investigation, Methodology, Writing—original draft; MZ: Formal analysis, Writing—review and editing, Supervision; JW: Resources, Writing—review and editing; All authors have read and agreed to the published version of the manuscript.

Funding

This work was supported by the National Natural Science Foundation of China (51568022), the Key Project of Jiangxi Natural Science Foundation (20202ACB202005), the National Natural Science Foundation of China (51869013), the Project of the Science and Technology of Jiangxi Education Department (GJJ210924), and the Key Laboratory of Hydraulic and Waterway Engineering of the Ministry of Education, Chongqing Jiaotong University (SLK2021B01).

Conflict of interest

The authors declare that the research was conducted in the absence of any commercial or financial relationships that could be construed as a potential conflict of interest.

Publisher's note

All claims expressed in this article are solely those of the authors and do not necessarily represent those of their affiliated organizations, or those of the publisher, the editors and the reviewers. Any product that may be evaluated in this article, or claim that may be made by its manufacturer, is not guaranteed or endorsed by the publisher.

References

Ahmed, A. (2015). Compressive strength and microstructure of softclay soil stabilized with recycled bassanite. *Appl. Clay Sci.* 104, 27–35. doi:10.1016/j.clay.2014.11.031

Aldaood, A., Bouasker, M., and Al-Mukhtar, M. (2014). Impact of wetting-drying cycles on the microstructure and mechanical proper-ties of lime-stabilized gypseous soils. *Eng. Geol.* 174, 11–21. doi:10.1016/j.enggeo.2014.03.002

Aqtash, Umaima Al, and Bandini, Paola (2015). Prediction of unsaturated shear strength of an adobe soil from the soil–water characteristic curve. *Constr. Build. Mater.* 98, 892–899. doi:10.1016/j.conbuildmat.2015.07.188

Bishop, A. W., and Blight, G. E. (1963). Some aspects of effective stress in saturated and partly saturated soils. *Géotechnique* 13 (3), 177–197. doi:10.1680/geot.1963.13.3.177

Chou, Y. L., and Wang, L. J. (2021). Soil-water characteristic curve and permeability coefficient prediction model for unsaturated loess considering freeze-thaw and dry-wet. *S&R.* 44 (1), 1–11. doi:10.28927/sr.2021.058320

Cui, S. L., and Si, D. D. (2014). Experimental research of swelling behaviors with initial water content and matric suction of bentonite–sand mixtures. *Geosystem Eng.* 17 (6), 317–324. doi:10.1080/12269328.2014.994788

Fredlund, D. G., Morgenstern, N. R., and Widger, R. A. (1978). The shear strength of unsaturated soils. *Can. Geotech. J.* 15 (3), 313–321. doi:10.1139/t78-029

Fu, H. Y., Liu, J., Zeng, L., Bian, H. B., and Shi, Z. N. (2019). Deformation and strength tests of pre-disintegrating carbonaceous mudstone under loading and soaking condition. *Rock Soil Mech.* 40 (4), 1273–1280. doi:10.16285/j.rsm.2017.2307

Han, B., Lu, G. Y., Zhu, Z. Q., Guo, Y. J., and Zhao, Y. W. (2019). Microstructure features of powdery coal-bearing soil based on the digital image measurement Technology and fractal theory. *Geotech. Geol. Eng. (Dordr).* 37 (3), 1357–1371. doi:10.1007/s10706-018-0691-8

Hassan Marwan Adil and Mohamad Ismail Mohd Ashraf (2018). Effect of soil types on the development of matric suction and volumetric water content for dike embankment during overtopping tests. *CivileJournal.* 4 (3), 668. doi:10.28991/cej-0309124

Huang, Gang, and Zheng, Mingxin (2021). Strength of vegetated coal-bearing soil under dry-wet cycles: An experimental study. *Int. J. Corros.* 2021,6657160 –13. doi:10.1155/2021/6657160

Jiang, Mingjing, Zhang, F., Hu, H., Cui, Y., and Peng, J. (2014). Structural characterization of natural loess and remolded loess under triaxial tests. *Eng. Geol.* 181, 249–260. doi:10.1016/j.enggeo.2014.07.021

Lin, Botao, and Amy, B. (2015). Shear strength of shale weathered expansive soils along swell-shrink paths: Analysis based on microscopic properties. *Environ. Earth Sci.* 74 (9), 6887–6899. doi:10.1007/s12665-015-4691-1

Ma, Shao-kun, Huang, M. s., Hu, P., and Yang, C. (2013). Soil-water characteristics and shear strength in constant water content triaxial tests on Yunnan red clay. *J. Cent. South Univ.* 20 (5), 1412–1419. doi:10.1007/s11771-013-1629-1

Miao, L. C., Yin, Z. Z., and Liu, S. Y. (2000). Research of the strength characteristics of UnsaturatedExpansive soils based on general tri-axial test. *J. Southeast Tuniversity Nat. Sci. Ed.* 30 (1), 121–125. in Chinese.

Nowamooz, H., Jahangir, E., Masrouri, F., and Tisot, J. P. (2016). Effective stress in swelling soils during wetting drying cycles. *Eng. Geol.* 210, 33–44. doi:10.1016/j.enggeo.2016.05.021

Qian, Zhai, Rahardjo, H., Satyanaga, A., Dai, G. l., and Du, Y. j. (2020). Effect of the uncertainty in soil-water characteristic curve on the estimated shear strength of unsaturated soil. *J. Zhejiang Univ. Sci. A* 21 (8), 317–330. doi:10.1631/jzus.a1900589

Sun, W.-J., and Cui, Y.-J. (2018). Investigating the microstructure changes for silty soil during drying. *Géotechnique* 68 (4), 370–373. doi:10.1680/jgeot.16.p.165

Wang, Yongwei, Li, K., Li, J., and Tang, S. (2021). Influence of soil particle size on the engineering properties and microstructure of a red clay. *Appl. Sci.* 11 (22), 10887. doi:10.3390/app112210887

Xiao, Xie, Li, P., Hou, X., Li, T., and Zhang, G. (2020). Microstructure of compacted loess and its influence on the soil-water characteristic curve. *Adv. Mater. Sci. Eng.* 2020, 1–12. doi:10.1155/2020/3402607

Xiong, C. R., Liu, B. C., and Zhang, J. S. (2005). Relation of matric suction with moisture state and density state of remolded cohesive soil. *Chin. J. Rock Mech. Eng.* 24 (2), 321–327. in Chinese.

Yang, Jikai, and Zheng, Mingxin (2018). Effects of density and drying-wetting cycle on soil water characteristic curve of coal soil. *J. East China Jiaot. Univ.* 35 (3), 91–96. in Chinese.

Zhang, Changguang, Zhao, Junhai, and Zhu, qian (2012). Classification and summary of shear strength for unsaturated soils. *J. Archit. Civ. Eng.* 29 (2), 74–82. in Chinese.

Zhang, Hong, Zhang, B., Wu, C., and Chen, K. (2021). Macro and micro analysis on coal-bearing soil slopes instability based on CFD-DEM coupling method. *PloS one* 16 (9), e0257362. doi:10.1371/journal.pone.0257362

Zhao, X. L., Zhang, C., Luan, Y., and Xiao, Z. (2018). Stereological analyses of microstructure of granular soils using the numerical method. *Bull. Eng. Geol. Environ.* 77 (3), 1103–1115. doi:10.1007/s10064-017-1086-4

Zhou, Cuiying, Cui, G., Liang, W., Liu, Z., and Zhang, L. (2021). A coupled macroscopic and mesoscopic creep model of soft marine soil using a directional probability entropy approach. *J. Mar. Sci. Eng.* 9 (2), 224. doi:10.3390/jmse9020224

Zuo, C. Q., Liu, D. G., Ding, S. L., and Chen, J. P. (2016). Micro-characteristics of strength reduction of tuff residual soil with different moisture. *KSCE J. Civ. Eng.* 20 (2), 639–646. doi:10.1007/s12205-015-0408-y